The *SIR2* gene family, conserved from bacteria to humans, functions in silencing, cell cycle progression, and chromosome stability

Carrie Baker Brachmann, Joyce M. Sherman,[1] Scott E. Devine, Elizabeth E. Cameron, Lorraine Pillus,[1] and Jef D. Boeke

Department of Molecular Biology and Genetics, Johns Hopkins School of Medicine, Baltimore, Maryland 21205; [1]Department of Molecular, Cellular and Developmental Biology, Porter Biosciences, University of Colorado, CB347, Boulder, Colorado 80309 USA

Genomic silencing is a fundamental mechanism of transcriptional regulation, yet little is known about conserved mechanisms of silencing. We report here the discovery of four *Saccharomyces cerevisiae* homologs of the *SIR2* silencing gene (*HSTs*), as well as conservation of this gene family from bacteria to mammals. At least three *HST* genes can function in silencing; *HST1* overexpression restores transcriptional silencing to a *sir2* mutant and *hst3 hst4* double mutants are defective in telomeric silencing. In addition, *HST3* and *HST4* together contribute to proper cell cycle progression, radiation resistance, and genomic stability, establishing new connections between silencing and these fundamental cellular processes.

[*Key Words*: *HST* genes; *Saccharomyces cerevisiae*; telomeric silencing; homologous recombination; chromosome segregation]

Received September 13, 1995; revised version accepted October 13, 1995.

Transcriptional inactivation of large genomic regions, or silencing, is an important and highly conserved mechanism of gene regulation. This regional, gene nonspecific form of repression is often associated with local alterations in chromatin structure. For example, heterochromatin is associated with transcriptional repression and has been well-documented at the *Drosophila* chromocenter and telomeres (Weiler and Wakimoto 1995), at mouse (Butner and Lo 1986) and *Schizosaccharomyces pombe* (Allshire et al. 1994; Nimmo et al. 1994) centromeres and telomeres, and on the mammalian inactive X chromosome (Migeon 1994). In *Drosophila*, breakpoints creating novel junctions between heterochromatic and euchromatic regions result in mosaic patterns of gene activity called position effect variegation (PEV). Finally, apparently *Bacillus subtilis* can exist with two chromosomes, only one of which is transcriptionally active (Schaeffer et al. 1976; Guillen et al. 1985).

In *Saccharomyces*, at least two types of genomic regions are silenced, telomeres and the silent *HM* mating-type loci. In both cases, silencing occurs independently of the gene being silenced, and displays an epigenetic or variegating component (Schnell and Rine 1986; Mahoney and Broach 1989; Pillus and Rine 1989; Gottschling et al. 1990; Sussel and Shore 1991; Sussel et al. 1993). Silenced loci are inaccessible to DNA modifying enzymes both in vivo and in isolated nuclei (Gottschling 1992; Singh and Klar 1992; Wright et al. 1992; Loo and Rine 1994), supporting the idea that silencing is associated with altered chromatin structure. Although *cis*-regulatory elements differ between the *HM* loci and telomeres, essential *trans*-acting factors are shared (Laurenson and Rine 1992). In particular, Sir2, Sir3, and Sir4 proteins are necessary for silencing, and participate with Rap1p and histones H3 and H4 in determining chromosomal structure and nuclear organization (for review, see Moretti et al. 1994; Shore 1994; Cockell et al. 1995; and Hecht et al. 1995). However, none of these interactions appear mediated through direct binding of Sir proteins to DNA (Buchman et al. 1988).

Recent data identifying mutations in subunits of the origin recognition complex (ORC; Bell et al. 1993) causing both silencing and cell cycle defects (Foss et al. 1993; Micklem et al. 1993; Loo and Rine 1994, 1995) point to direct mechanistic connections between DNA replication and silencing. Similarly, recent experiments suggest that delays in cell cycle progression can influence silencing (Laman et al. 1995) and that the G_2/M transition may represent a particularly vulnerable time for factors to activate silenced chromatin (Aparicio and Gottschling 1994). Exactly how the *SIR* genes, ORC, *cis*-regulatory regions, and other factors work together to promote transcriptional silencing is not yet clear.

Like the other *SIR* genes, *SIR2* shares an essential

function in silencing both at the *HM* loci and telomeres, yet in particular, *SIR2* has several unique and distinguishing characteristics. *SIR2* suppresses rDNA recombination (Gottlieb and Esposito 1989) and may participate in regulation of histone deacetylation (Braunstein et al. 1993).

We and others (Derbyshire et al. 1995) have discovered a gene family in *Saccharomyces cerevisiae* with homology ranging from 30% to 63% amino acid identity with *SIR2*. In our search for *SIR2* homologs we have also identified potential homologs from a bacterium as well as from plants and mammals. None of the yeast *HST* genes (homologous to SIR2) result in a Sir$^-$ reduced mating phenotype when mutated. However, increasing *HST1* gene dosage significantly restores silencing to a *sir2* mutant, and a *hst3 hst4* double mutant is defective in telomeric silencing. These results indicate that although *HST* genes are not fully redundant with *SIR2*, they can participate in silencing.

We have also determined that the *hst3 hst4* double mutant has a number of defects in addition to those affecting telomeric silencing. In this strain, cells accumulate with G_2 DNA content at the G_2/M boundary. The interaction of *hst3 hst4* mutations with the checkpoint control mutation *rad9* was examined and a dramatic synthetic UV sensitivity phenotype was observed. We find that the *hst3 hst4* double mutant exhibits significantly elevated rates of mitotic recombination, and chromosome missegregation. These phenotypes indicate that in addition to telomeric silencing, Hst3p and Hst4p play important roles in the cell cycle, DNA damage control, recombination, and genomic maintenance. The discovery and characterization of the conserved *SIR2* gene family suggests that silencing proteins, first identified in yeast, may have general functions in cell cycle progression and genomic integrity.

Results

Identification of a novel family of yeast HST *genes homologous to* SIR2

We have discovered four new members of a *SIR2* gene family through a combination of strategies including low-stringency hybridization, degenerate PCR, and data base analysis. These *Saccharomyces* genes encode proteins closely related by amino acid sequence. We have determined by Northern blot analysis using gene-specific probes that all of the *HST* genes are expressed (data not shown). None of the *HST* genes are essential; *S. cerevisiae* with complete knockouts in any of these genes, whether singly or in combination (including the quintuple null *sir2 hst1 hst2 hst3 hst4* mutant), is viable. However, some synthetic phenotypes are observed with various null mutant combinations and are described below.

The *SIR2* gene family also includes related sequences in a variety of eukaryotes (human, rat, mouse, *Caenorhabditis elegans*, *Arabidopsis*, and fission yeast) and the prokaryote *Staphylococcus aureus*. Figure 1A shows an alignment of the five *S. cerevisiae* protein sequences as well as homologs from the budding yeast *Kluyveromyces lactis* (Chen and Clark-Walker 1994), *S. aureus*, *Rattus norvegicus*, and *Homo sapiens* (see Materials and methods for details of sequence discovery and isolation). There are several highly conserved domains within the family, in particular the region that we have defined as the core domain (bounded by arrowheads in Fig. 1A). Although the core domain is well-conserved among family members, the relative lengths of the terminal domains of these proteins is quite variable (Fig. 1B). Alignment of the yeast proteins with homologs from other species reveals three subfamilies. One consists of Sir2p, Hst1p, and *K. lactis* Sir2p, and has a long, partially conserved amino-terminal domain. The second contains Hst2p and the mammalian and *C. elegans* sequences and the third contains Hst3p and Hst4p.

Conserved amino acid sequence features of Sir2 and the Hst proteins

Two amino acid sequence motifs are diagnostic for the Sir2 protein family: GAGISTS(L/A)GIPDFR and YTQNID. These amino acid coding regions formed the basis for degenerate PCR primers (Fig. 1A) and should be useful for identifying additional family members, should any exist. There are a number of other amino acid motifs revealed by the multiple sequence alignment. A previous study (Chen and Clark-Walker 1994) noted that Sir2p and KlSir2p contain motifs typical of DNA-binding proteins. Specifically, they contain a cluster of cysteine residues with unique spacing suggestive of a zinc finger and two potential leucine zippers. The four cysteine residues of the proposed metal-binding motif are conserved in all of the *HST* sequences (Fig. 1A, asterisks) and suggest that these residues may be functionally important. Although at least one leucine zipper may also be present in *S. aureus* Sir2p (SaSir2p), Hst2p, and Hst3p, it is interesting to note that the two putative leucine zipper motifs are conserved only in the most Sir2p-like family members—namely Sir2p itself, KlSir2p, and Hst1p. Many DNA-binding proteins contain these motifs.

HST1 *overexpression restores silencing at* HMR

Single *hst* null mutants, as well as *hst3 hst4* null mutants mate as well as wild type, in both *MAT***a** and *MAT*α backgrounds, indicating normal *HM* locus silencing in these strains. To determine whether the *HST*s share functional similarity with *SIR2*, the ability of the Hst proteins when overexpressed to complement the mating defect in a *sir2* null mutant background was tested. The *MAT***a** and *MAT*α *sir2* strains LPY11 and LPY1393, respectively (see Table 1 for strain descriptions), were transformed with 2μ plasmids carrying *HST1*, *HST2*, *HST3*, or *SIR2*. Equal numbers of cells from logarithmically growing cultures of the LPY11 and LPY1393 transformants were spotted onto lawns of the mating tester strains LPY143 and LPY142, respectively (*MAT*α and *MAT***a**). Overexpression of *HST1* (Fig. 2), but not of *HST2* or *HST3* (data not shown), complemented the *sir2* mu-

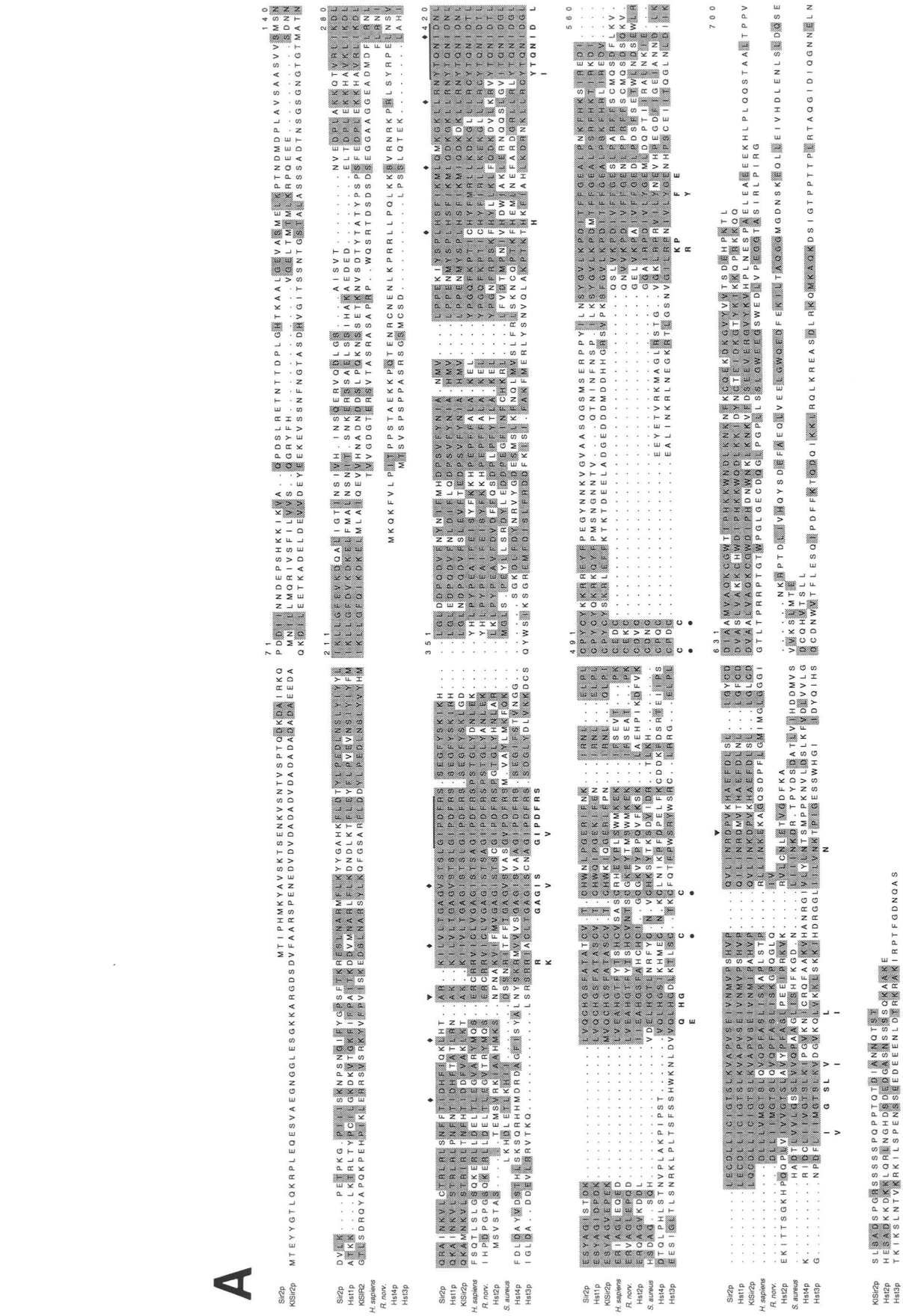

Figure 1. (*See facing page for B and legend.*)

tation. Interestingly, complementation was specific to the *MAT*α background.

To determine the extent to which *HST1* is able to complement the mating defect caused by *sir2*, standard quantitative mating assays were performed (Sprague 1991). The mating efficiencies of LPY11 and LPY1393 transformed with vector alone or with constructs overexpressing either *HST1* or *SIR2* were determined. The values presented in Figure 2 represent the average mating efficiencies obtained for at least two independent transformants. The mating efficiency of LPY1393 is ≥5000-fold above background when *HST1* is overexpressed. However, it is still ~30-fold lower than LPY1393 transformed with a *SIR2* plasmid. Consistent with the qualitative mating results (Fig. 2), no significant complementation of the *sir2* mating defect by high copy *HST1* was detected in the *MAT***a** background.

HST1 could act to restore mating to a *sir2* strain directly by functioning in transcriptional silencing or indirectly by influencing other events in the mating pathway. To test whether high copy *HST1* suppression of the *sir2* mating defect is attributable to partial restoration of transcriptional silencing, a *sir2* strain with a $SUP3_{am}$ reporter gene at *HMR* (LPY1539) was constructed. In this strain, the **a** information normally present at *HMR* has been replaced with the gene encoding an amber suppressor tRNA (Schnell and Rine 1986). Because this strain also contains a $trp1_{am}$ mutation, growth on plates without tryptophan reflects transcription of the $SUP3_{am}$ gene at *hmr* (Fig. 2B). The *sir2* mutant strain grows well in the absence of tryptophan. In contrast, when these cells are transformed with the *HST1* or *SIR2* high copy plasmids, they exhibit significantly decreased growth, presumably attributable to restored silencing of the $hmr\Delta::SUP3_{am}$ reporter. Thus, Hst1p not only shares sequence homology with Sir2p, but also has silencing function.

Telomeric silencing in hst *mutants*

SIR2 function is necessary for telomeric silencing; therefore, we tested the *hst* mutants for defects in telomeric position effect. The assay uses a *URA3* gene integrated at the subtelomeric *ADH4* locus on chromosome IV (ADH4UCA-IV; Aparicio et al. 1991). In wild-type cells the subtelomeric *URA3* is expressed stochastically, with a small portion of the population expressing *URA3* and a majority of the population silencing its expression. When plated onto 5-fluoro-orotic acid (5-FOA) medium, wild-type cells survive due to this silencing. Strains unable to silence the expression of telomeric *URA3*, such as *sir2* strains, will not grow on 5-FOA medium. By comparing growth of strains on permissive medium to growth on 5-FOA, one can estimate the extent to which a mutant strain has lost the ability to repress transcription of the telomeric *URA3* (Fig. 3). Consistent with previous experiments, *sir2* cells were unable to grow on 5-FOA, indicating loss of telomeric silencing. In contrast, the telomeric *URA3* gene was repressed comparably in wild-type, *hst1*, *hst2*, and *hst4* strains (Fig. 3, cf. row B with C, D, and F), indicating no defect in telomeric silencing in these strains. The *hst3* mutant and wild-type strains had a similar frequency of Foa^R cells, but the *hst3* colonies grew much slower than wild type (Fig. 3, cf. row B with E). Strikingly, the *hst3 hst4* double mutant showed significantly greater 5-FOA sensitivity than either single mutant alone (Fig. 3, cf. row G with B, E, and F), and the number of Foa^R cells is reduced ~100-fold relative to wild-type. We conclude that *HST3* and *HST4* play important roles in telomeric silencing. The synergy between *hst3* and *hst4* mutations is explored further in the phenotypic characterization below.

The hst3 hst4 *double mutant is temperature sensitive, has low viability, and altered cell cycle distribution*

We discovered that the *hst3 hst4* strain is temperature sensitive (Ts) for growth at 37°C. In contrast to the *hst3* and *hst4* single mutants, and the *hst3 hst4* double mutant maintaining a centromeric *HST3* plasmid, *hst3 hst4* cells formed colonies at 37°C at efficiencies 37-fold to >1000-fold lower than wild type (data not shown). When

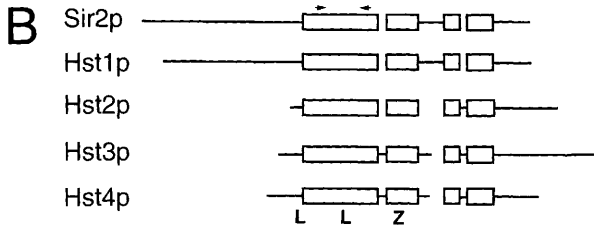

	Sir2p	Hst1p	Hst2p	Hst3p
Hst1p	**63** / 76	------	% amino acid identity / % amino acid similarity	
Hst2p	**34** / 56	**35** / 55	------	
Hst3p	**32** / 54	**31** / 56	**25** / 49	------
Hst4p	**29**/ 51	**27** / 50	**28** / 52	**35** / 56

Figure 1. Alignment of yeast Hst proteins and related sequences from other species. (*A*) Amino acid sequence alignment. (●) Cysteine residues of the putative metal binding domain; (♦) leucine residues of the putative leucine zippers; (▼) boundaries of the core domain; (solid line) sites of degenerate PCR primers used. Shaded residues are those that are identical or similar based on the Blosum 62 matrix; residues in bold below alignment are absolutely conserved in known family members. Alignment was performed using PILEUP; amino acids 477–490 were adjusted manually to align putative metal-binding domain. *SIR2* homologs from species other than yeast are included (see Materials and methods). (*B*) Block diagram of the yeast Hst proteins and Sir2p. The yeast proteins are compared based on the alignment in *A* with open boxes indicating regions of similarity to Sir2p. Table contains pairwise comparisons between family members calculated by GAP using preset options. The nucleotide sequences of *HST1*, *HST2*, and *HST3* have been submitted to the GenBank data library under accession nos. U39041, U39063, and U39062, respectively. *HST4* is encoded by the cosmid under accession no. Z48784.

Table 1. *Yeast strains*

Strain	Genotype
LPY11[a]	*MAT***a** *ade2-1 can1-100 his3-11 leu2-3,112 trp1-1 ura3-1 GAL sir2Δ::HIS3*
LPY1393[a]	*MATα ade2 his3 leu2 sir2Δ::HIS3 ura3*
LPY142	*MAT***a** *his4*
LPY143	*MATα his4*
LPY1539	*MATα ade2 his3 leu2 trp1*$_{am}$ *ura3 sir2Δ::HIS3 hmrΔ::SUP3*$_{am}$
YPH499,500 and derivatives	
YPH499	*MAT***a** *ura3-52 his3Δ200 leu2Δ1 trp1Δ63 ade2-101 lys2-801*
YPH500	*MATα ura3-52 his3Δ200 leu2Δ1 trp1Δ63 ade2-101 lys2-801*
YCB506	isogenic to YPH499 *hst3Δ3::HIS3 hst4Δ1::URA3*
YCB538	isogenic to YPH499 *hst3Δ3::HIS3 hst4Δ1::URA3*
YCB547	isogenic to YPH500 *hst3Δ3::HIS3 hst4Δ1::URA3*
X23-9A	isogenic to YPH500 *hst4Δ1::URA3*
X23-10D	isogenic to YPH500 *hst3Δ3::HIS3*
YCB405	isogenic to YPH499 *hst3Δ3::HIS3*
YPH279	*MAT***a**/α *ura3-52/ura3-52 HIS3/his3Δ200 leu2Δ1/leu2Δ1 TRP1/trp1Δ1ade2-101/ade2-101 lys2-801/lys2-801 CFVII(RAD2.d.YPH277)URA3 SUP11*
YCB654	*MAT***a**/α *ura3-52/ura3-52 his3Δ200/his3Δ200 leu2Δ1/leu2Δ1 trp1Δ63/trp1Δ63 ade2-101/ade2-101 lys2-801/lys2-801 hst3Δ3::HIS3/hst3Δ3::HIS3 hst4Δ1::URA3/hst4Δ1::URA3 CFVII(RAD2.d.YPH277)TRP1 SUP11*
YCB657	*MAT***a**/α *ura3-52/ura3-52 his3Δ200/his3Δ200 leu2Δ1/leu2Δ1 trp1Δ63/trp1Δ63 ade2-101/ade2-101 lys2-801/lys2-801 hst3Δ3::HIS3/hst3Δ3::HIS3 hst4Δ1::URA3/hst4Δ1::URA3 CFVII(RAD2.d.YPH277)TRP1 SUP11*
YCB684	isogenic to YPH500 *hst3Δ3::HIS3 CFVII(RAD2.d.YPH277)TRP1 SUP11*
YCB624	isogenic to YPH499 *rad9Δ1::TRP1*
YCB627	isogenic to YPH500 *hst3Δ3::HIS3 hst4Δ1::URA3 rad9Δ1::TRP1*
YCB632	isogenic to YPH500 *rad9Δ1::TRP1 hst4Δ1::URA3*
YCB633	isogenic to YPH500 *rad9Δ1::TRP1 hst3Δ3::HIS3*
FY2 derivatives[b]	
YPH681	*MAT***a** *ura3-52 his3Δ200 leu2Δ1 trp1Δ63 lys2Δ202*
YPH680	*MATα ura3-52 his3Δ200 leu2Δ1 trp1Δ63 lys2Δ202*
YCB470	isogenic to YPH681 *hst3Δ3::TRP1*
YCB575	isogenic to YPH681 *hst4Δ1::TRP1*
YCB600	isogenic to YPH681 *hst3Δ3::TRP1 hst4Δ1::TRP1* pCAR202
YCB600$^-$	isogenic to YPH681 *hst3Δ3::TRP1 hst4Δ1::TRP1*
YCB601	isogenic to YPH680 *hst3Δ3::TRP1 hst4Δ1::TRP1* pCAR202
YCB601$^-$	isogenic to YPH680 *hst3Δ3::TRP1 hst4Δ1::TRP1*
YCB669	isogenic to YPH681 YCp50
YCB674	isogenic to YPH681 *hst3Δ3::TRP1 hst4Δ1::TRP1* pCAR202 YCp50
YCB674$^-$	isogenic to YPH681 *hst3Δ3::TRP1 hst4Δ1::TRP1* YCp50
YCB647	isogenic to YPH681 *leu2Δ::TRP1 ADH4::URA3–TEL*
YCB648	isogenic to YPH681 *hst1Δ3::TRP1 ADH4::URA3–TEL*
YCB649	isogenic to YPH681 *hst2Δ2::TRP1 ade2Δ1 ADH4::URA3–TEL*
YCB650	isogenic to YPH681 *hst3Δ3::TRP1 ADH4::URA3–TEL*
YCB651	isogenic to YPH681 *hst4Δ1::TRP1 ADH4::URA3–TEL*
YCB652	isogenic to YPH681 *sir2Δ2::TRP1 ADH4::URA3–TEL*
YCB653	isogenic to YPH681 *hst3Δ3::TRP1 hst4Δ1::TRP1 ADH4::URA3–TEL*
YCB692	isogenic to YPH681 *ade2::hisG::URA3::hisG*
YCB693	isogenic to YPH681 *hst3Δ3::TRP1 ade2::hisG::URA3::hisG*
YCB694	isogenic to YPH681 *hst4Δ1::TRP1 ade2::hisG::URA3::hisG*
YCB695	isogenic to YPH681 *hst3Δ3::TRP1 hst4Δ1::TRP1 ade2::hisG::URA3::hisG* pCAR202
YCB695$^-$	isogenic to YPH681 *hst3Δ3::TRP1 hst4Δ1::TRP1 ade2::hisG::URA3::hisG*

[a]These strains are derived from W303.
[b]YPH680 and YPH681 are derived from the FY2 series of strains (Winston et al. 1995).

the *hst3 hst4* cells that grow at high temperature were restreaked at 37°C, they maintained their Ts$^+$ phenotype (data not shown). Thus, we believe that the variability in frequency of Ts$^+$ cells is attributable to sporadic acquisition of suppressors. Because these suppressors can accumulate, many of the experiments performed on *hst3 hst4* strains were carried out using strain YCB600$^+$, which carries an *HST3 CEN* plasmid. The plasmid is segregated just before the experiment, generating YCB600$^-$, to minimize the accumulation of suppressors.

Microscopically we observed that most of the mutant cells were larger than wild type (Fig. 4), and that a log-phase culture of an *hst3 hst4* strain contained more large-budded cells than wild-type, a phenotype exacerbated at higher temperatures (Fig. 5A). In this large-budded population the daughter cell was often as large as the mother, a form rarely observed in wild-type cultures (Fig.

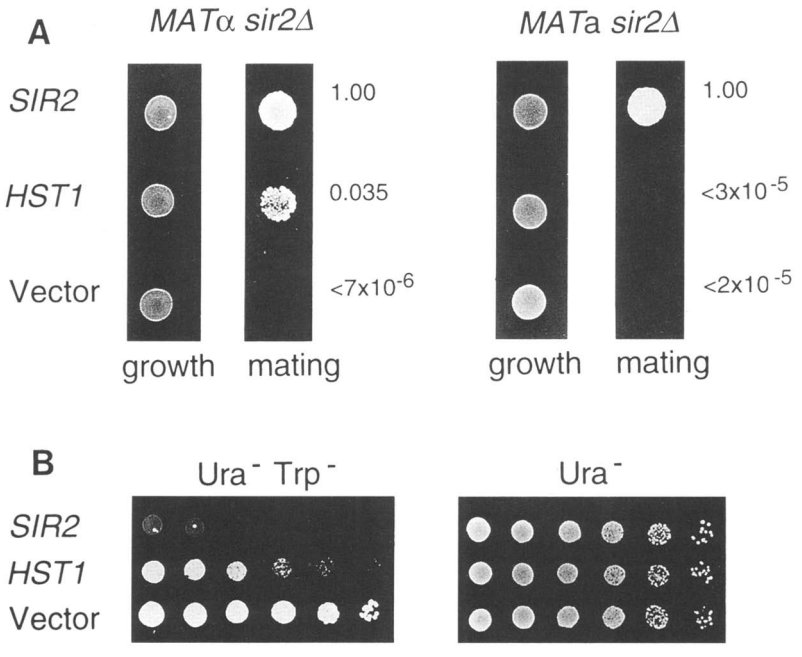

Figure 2. *HST1* restores silencing at *HMR* in *sir2* mutants. (*A*) Increased *HST1* gene dosage was tested for ability to complement *MAT***a** and *MAT*α *sir2* mating defects. Comparisons to 2μ vector and a *SIR2* 2μ plasmid are shown. Approximately equal numbers of each transformant were spotted onto SC–Ura to assay growth and onto lawns of the mating testers LPY142 and LPY143 to assay mating. The mating efficiencies determined by quantitative mating assays are also presented. The values represent the average mating efficiency of at least two independent isolates for each transformant. (*B*) To determine whether the observed complementation is attributable to restoration of transcriptional silencing at *HMR*, a *sir2* strain with a $SUP3_{am}$ reporter gene at *HMR* and a $trp1_{am}$ mutation (LPY1539) was transformed with the 2μ plasmids. Transformants were assayed for Trp expression by spotting serial dilutions onto SC–Ura–Trp and for growth by spotting on SC–Ura plates.

4). Because cells with large buds indicate a block in mitosis, we examined DNA content by flow cytometry (Fig. 5B). The double mutant strain exhibited a dramatic increase in the number of cells with G_2 DNA content. Both single mutants (*hst3* and *hst4*) are similar to wild type microscopically and by flow cytometry (Fig. 5; data not shown). To determine the nuclear morphology of the *hst3 hst4* mutant strain, we visualized nuclei with the fluorescent dye DAPI. We found that the double mutant showed an increase in the percentage of large-budded cells with the nucleus at or across the neck (Figs. 4 and 5A), but that the percentage of large-budded cells in which the nucleus had divided was similar to wild-type.

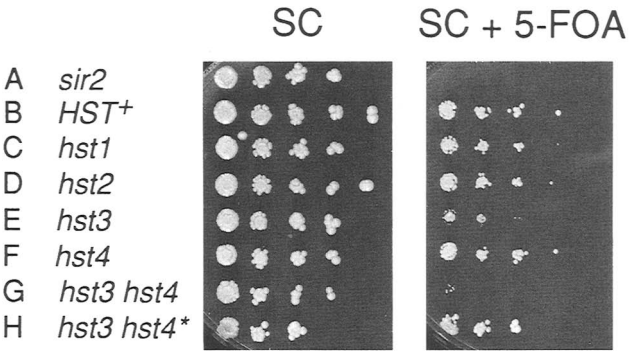

Figure 3. The *hst3 hst4* mutant shows increased expression of a telomeric *URA3* gene. Tenfold serial dilutions were plated onto either SC medium or SC containing 0.1% 5-FOA. Strains used were: (A) YCB652; (B) YCB647; (C) YCB648; (D) YCB649; (E) YCB650; (F) YCB651; (G) YCB653; and (H) YCB600$^-$. Strains A–G contain a telomeric copy of *URA3* at *ADH4* (*ADH4::URA3–TEL*), strain H does not. The 5-FOA sensitivity of the *hst3 hst4 ADH4::URA3–TEL* strain is not attributable to a general 5-FOA supersensitivity because *hst3 hst4 ura3* strains lacking telomeric *URA3* grow normally on 5-FOA (row H).

Therefore, the *hst3 hst4* strain contains a larger fraction of cells in which the DNA has been replicated but cell division has not occurred.

This accumulation could be the result of a G_2/M delay, or it could be attributable to the irreversible arrest of a subpopulation of the *hst3 hst4* mutant cells. To distinguish between these two possibilities we determined the viability of the double mutant cells (Table 2). Whereas the viability of the *hst3* and *hst4* single mutants was similar to wild type, we observed that 44% of double mutant cells were inviable. This defect was completely corrected by the presence of the *HST3* CEN plasmid. Strikingly, when we determined the viability of the *hst3 hst4* large-budded cell population, we found that only 27% of these cells were viable, as opposed to 89% in wild type. Thus, it appears that the large-budded cell population in the mutant has two components, a normal component and a larger inviable component lacking in the wild-type population.

By microscopic examination of manipulated cells grown at 37°C, we determined that the majority of the *hst3 hst4* large-budded cells that died did so as 2- or 4-cell bodies (of equal size), whereas a few formed microcolonies of 5–20 cells (data not shown). Many of these dead cells were bloated and misshapen. The large-budded cell inviability observed in the *hst3 hst4* double mutant suggests that the G_2/M accumulation observed in the double mutant reflects the existence of a subset of ultimately inviable cells that are arrested at this juncture of the cell cycle, rather than a cell-cycle delay.

The hst3 hst4 rad9 *strain is hypersensitive to UV irradiation*

The excess G_2/M cells observed in the *hst3 hst4* double mutant strain could result from DNA damage triggering

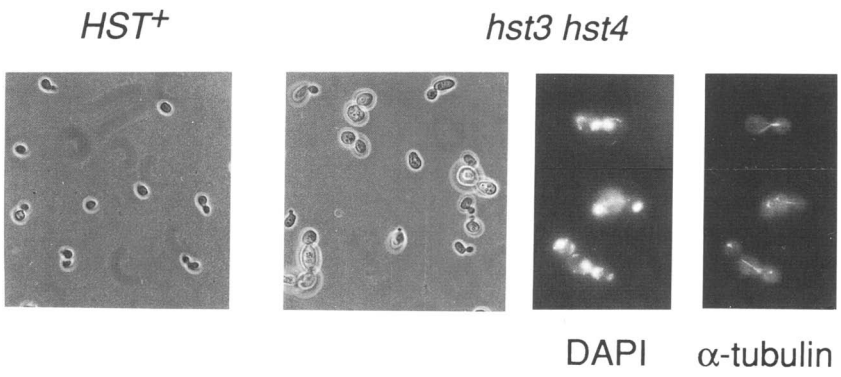

Figure 4. Aberrant morphology of *hst3 hst4* mutants. Log phase cells of wild type (YPH681) and mutant (YCB600$^-$) strains were visualized by phase contrast. Note increased number of large-budded cells and increased cell size in mutant culture. Also shown are representative aberrant nuclear and microtubule morphologies of the mutant.

a *RAD9*-dependent delay. Thus, we examined the effect of introducing a *rad9* mutation into these strains. The prediction of this model is that a triple mutant (*hst3 hst4 rad9*) would lose the G_2/M accumulation (or lose viability). The triple mutant grows like the *hst3 hst4* double mutant, and like the *hst3 hst4* mutant, exhibits a G_2/M accumulation, indicating that this accumulation is not *RAD9* dependent.

We examined the sensitivity of these strains to UV irradiation. The *hst3 hst4* double mutant showed a modest UV-irradiation sensitivity, similar to that of *rad9* alone (Fig. 6). *rad9* cells die when UV irradiated because they do not have time to repair DNA damage, but this lethality can be alleviated by inducing a G_2/M delay (Weinert and Hartwell 1988). Accordingly, if the increased G_2/M accumulation in *hst3 hst4* cells results from a reversible cell-cycle delay at a point similar to a *RAD9* checkpoint, in theory *hst3 hst4* could rescue the UV sensitivity of *rad9* cells. When we tested the *hst3 hst4 rad9* mutant for UV resistance, we in fact found that the triple mutant is UV hypersensitive relative to either parent (Fig. 6). The synergistic effects of *hst* mutations and *rad9* are reminiscent of the connection between silencing (*SIR3*) and DNA repair/checkpoint control (*RAD7*) pathways (Paetkau et al. 1994).

hst3 hst4 *mutants display increased chromosome loss and recombination*

Many mutant strains that exhibit an accumulation of G_2/M cells lose chromosomes at an increased rate (Gerring et al. 1990; Doheny et al. 1993). We tested the *hst3 hst4* double mutant for chromosome stability using an artificial chromosome and a visual ploidy assay (Spencer et al. 1990; Shero et al. 1991). Our analysis made use of two marked chromosome fragments (derived from two different native yeast chromosomes), which result in a white colony in an *ade2* background; colonies lacking the marked fragment are red (Hieter et al. 1985). Using this assay we observed that the *hst3 hst4* strain showed high-frequency sectoring with both chromosome fragments. In addition, the *hst3* mutant exhibited a modest increase in sectoring, whereas the *hst4* mutant was indistinguishable from wild type.

The frequency of loss of one such fragment was calculated in diploid strains in which the dosage of the frag-

A

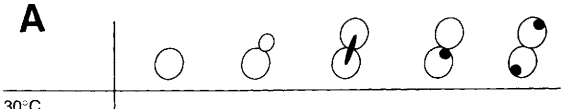

30°C					
HST+	48%	39%	1%	0%	12%
hst3 hst4	36%	41%	11%	4%	9%
30°C → 37°C					
HST+	57%	33%	1%	1%	9%
hst3 hst4	17%	23%	19%	38%	4%

B

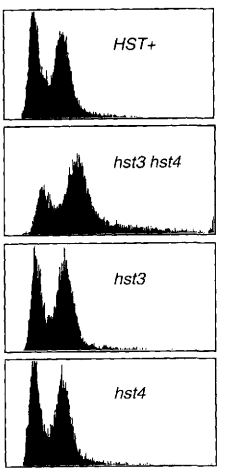

Figure 5. Altered cell cycle distribution in *hst3 hst4* mutant cells. (*A*) Morphological analysis. Log phase cultures in YPD were fixed and stained with DAPI to visualize nuclei. Similar results were obtained in two separate experiments. The temperature shift experiment was performed by collecting log phase cells from 30°C YPD cultures, resuspending them in prewarmed 37°C YPD, and incubating them for 4.5 hr at 37°C before analysis. At 37°C, a number of large-budded mutant cells appear to have budded a third time, and in some cases a fourth (data not shown). Strains used were YPH499 and YCB506. (*B*) FACScan analysis. Log phase cultures were analyzed by flow cytometry. Number of cells is shown on the y-axis, and fluorescent intensity of emitted light is shown on the x-axis. The slight x-axis shift seen in the double mutant is likely caused by its increased cell size. Strains used were YPH499, YCB538, X23-10D, and X23-9A.

Table 2. *Viability measurements*

Strain	Relevant genotype	Percent viability[a] (all cells)	Percent viability (large-budded cells)	Percent large-budded cells[b]
YPH680	*HST*$^+$	89	89	26
YCB470	*hst3*	96	82	18
YCB575	*hst4*	100	100	14
YCB601	*hst3 hst4* [*HST3 CEN*]	88	79	18
YCB601$^-$	*hst3 hst4*	44	27	56

[a]Viability was determined by micromanipulation and growth of individual cells on YPD at 30°C.
[b]Defined as cells in which daughter cell is >50% the size of mother cell.

ment can be assessed. A single copy of the chromosome fragment in an *ade2–101* homozygote results in pink colonies, whereas colonies containing two (or more) copies of the fragment are white. This assay allows the rate of chromosome missegregation to be calculated, and differentiates between chromosome loss (1:0 segregation) and chromosome nondisjunction (2:0 segregation) events. A 1:0 missegregation event in the first division results in a half red/half pink sectored colony; similarly, a half red/half white sectored colony is the result of a 2:0 missegregation event. The *hst3 hst4/hst3 hst4* double mutant exhibited a dramatic chromosome missegregation rate of 35-fold above the wild type (Table 3). Nondisjunction events (46-fold elevated) were somewhat more frequent than chromosome loss events (25-fold elevated). The *hst3/hst3* homozygote showed a modest missegregation rate increase of less than twofold over the wild-type homozygote (Table 3). We also examined the rate of loss of the small circular plasmid YCp50 in wild-type and mutant strains. We found that in the *hst3 hst4* mutant the rate of plasmid loss was elevated 2.6-fold above wild type (Fig. 7). Thus, the stability of both plasmids and chromosome fragments is reduced in the *hst3 hst4* mutant, but the much larger chromosome fragments show a more stringent requirement for the *HST* genes.

Homologous recombination frequency provides another insight into genomic stability. We examined recombination frequency using two assays. The first uses an *hst3 hst4/hst3 hst4 CAN1*^{S}*/can1*^{R} strain. Because the *CAN1*^{S} allele is dominant, it renders diploid cells sensitive to canavanine. If the *CAN1*^{S} allele is lost, generally by gene conversion of the *CAN1*^{S} allele to *can1*^{R}, cells become resistant to canavanine (Can^R). The *hst3 hst4* mutants exhibited an increase in the frequency of Can^R cells relative to wild type. Can^R cells can result from loss of chromosome V, leaving the cell with a single *can1*^{R} allele, or from recombinational homozygosis. Because the observed increase in frequency in Can^R cells is complicated by the fact that the *hst3 hst4* mutant has a chromosome segregation defect, we designed a second assay using the *ADE2* disrupter pΔADE2 (Aparicio et al. 1991). When integrated at *ADE2*, this construct replaces part of *ADE2* with direct repeats of *hisG* flanking *URA3*. We integrated this *ade2::hisG::URA3::hisG* construct into our mutant haploid strain, selected Ura$^+$ cells, and allowed the resultant Ade$^-$ (pink) cells to grow on medium containing uracil. We then asked how many cells had become Foa^R by recombination between the repeated *hisG* sequences. We observed a fivefold increase in mitotic recombination in *hst3 hst4* strains relative to wild type, and more modest increases in the single mutants (Table 4). Thus, in addition to playing roles in silencing, proteins of the Sir2p family affect chromosome stability and recombination, indicating a more general role in chromatin metabolism.

Discussion

The SIR2 *gene family*

Members of the yeast *SIR2* gene family we have discovered range from 29% to 63% identical to Sir2p overall at

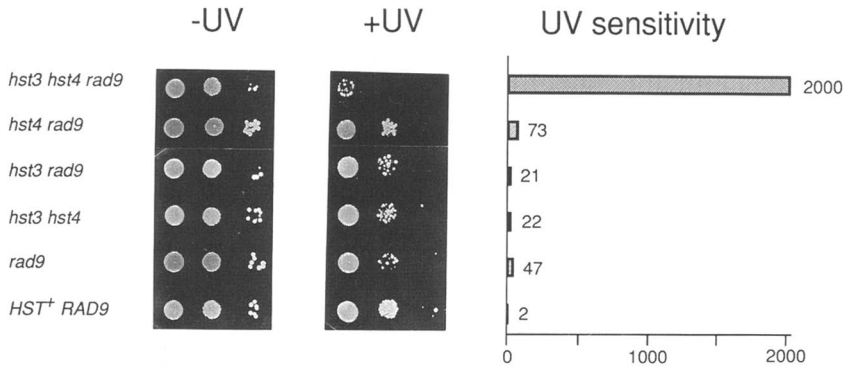

Figure 6. UV sensitivity of the *hst3 hst4* double mutant and hypersensitivity of the *hst3 hst4 rad9* triple mutant. Five microliters of 100-fold serial dilutions were spotted onto YPD plates and either UV irradiated with 80 J/m^2 using a Stratalinker (Stratagene; setting of 80 μJ×100/cm^2) immediately and again 12 hr later (+UV) (Weinert et al. 1994), or left unirradiated (−UV). Plates were wrapped in foil to prevent photoreactivation and incubated at 30°C. The bar graph depicts the results numerically as UV sensitivity (number of cells exposed to UV/number of cells surviving UV exposure). Strains used, from top to bottom, were YCB627, YCB632, YCB633, YCB547, YCB624, and YPH500.

Table 3. *Chromosome fragment loss rates*

Strain	Genotype	Chromosome mis-segregation rate	Percent 1:0 events[a]	Percent 2:0 events[b]	No. of colonies with 1 CF[c]
YPH279	*HST*$^+$/*HST*$^+$	0.06	0.03	0.03	29046[d]
YCB405 × YCB684	*hst3/hst3*	0.11	0.053	0.053	1900
YCB654	*hst3 hst4/hst3 hst4*				
	a	1.41	0.28	1.13	708
	b	2.48	1.14	1.34	968
YCB657	*hst3 hst4/hst3 hst4*				
	a	2.09	0.91	1.18	1102
	b	2.5	0.66	1.84	760
Mean ± S.D.	*hst3 hst4/hst3 hst4*	2.12 ± 0.51	0.75 ± 0.37	1.37 ± 0.32	

The above strains were plated for single colonies, and half-sectored colonies (at least 50% red) were counted. YCB654 and YCB657 are isogenic diploids, and a and b denote duplicate experiments for each. The final line shows the mean of the four *hst3 hst4/hst3 hst4* experiments and indicates the standard deviation. Number of half sectored colonies scored: YCB654a (10); YCB654b (24); YCB657a (23); YCB657b (19); YCB405 × YCB684 (2).

[a]Number of red/pink half-sectored colonies divided by total colonies with one chromosome fragment (CF).

[b]Number of red/white half-sectored colonies divided by total colonies with one CF.

[c]The total colonies with one CF.

[d] From Gerring et al. (1990).

the amino acid level with most variation occurring in the length and sequence of their amino and carboxyl termini. All the *HST*s contain an even more highly conserved core region that includes several absolutely conserved motifs of unknown function, four completely conserved cysteines hypothesized to form a zinc finger and a partially conserved putative leucine zipper domain. The zinc finger and leucine zipper motifs suggest that these proteins may form complexes with other proteins and bind to DNA. Consistent with this is the hypersensitivity to DNA-targeting drugs of *sir2* mutants in *K. lactis* (Chen and Clark-Walker 1994) and the UV hypersensitivity reported here. However, there is as yet no evidence that Sir2p or the Hst proteins bind DNA.

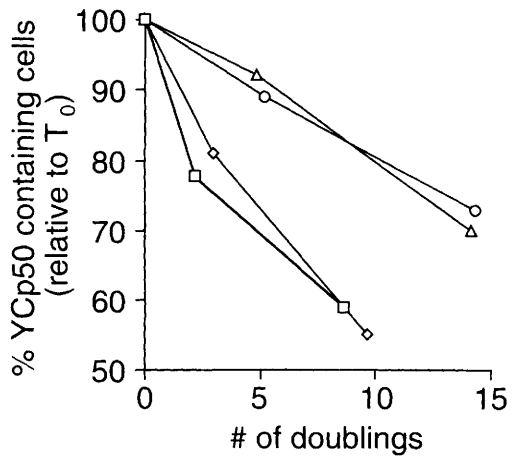

Figure 7. Elevated loss of a CEN plasmid in *hst3 hst4* mutant cells. Mutant strains show an average loss rate 2.6-fold greater than wild-type strains (Dani and Zakian 1983). Log phase cultures selecting for the CEN plasmid YCp50 were diluted into YPD and grown nonselectively for the number of generations indicated. Cells were plated on YPD and selective plates to determine the number of cells that had lost the plasmid. The results depict two YCp50 transformants each for YCB674$^-$ (□ and ◇) and YCB669 (○ and △) normalized to percentage of plasmid-bearing cells in selective cultures at time 0 (84% and 89% for *HST*$^+$, 73% and 81% for *hst3 hst4*).

HST *genes have silencing functions*

The *HST*-encoded proteins exhibit both remarkable sequence similarity to Sir2p as well as functional overlap. Hst1p is Sir2p's closest relative. It is 63% identical to Sir2p overall and 82% identical in the conserved core. *HST1* is not normally required for silencing at either the *HM*-type loci or telomeres as an *hst1* strain mates and maintains normal levels of telomeric repression. However, we have shown that, in a novel instance of mating-type specific suppression, overexpression of *HST1* restores significant mating competence to a *MAT*α *sir2* strain. That this is attributable to a restoration of silencing at *HMR* is demonstrated by the reduction in expression of *HMR*-located $SUP3_{am}$. A possible explanation for *HST1*'s α-specific complementation of the *sir2* mating defect may lie in the fact that repression is reestablished more readily with an *HMR* than with an *HML* silencer element (Shei and Broach 1995) and that the function of *HST1* may be to facilitate the establishment of repression at *HMR*.

Significantly, we have shown that expression of a telomeric *URA3* gene is derepressed in an *hst3 hst4* mutant strain. Although not as extreme as the *sir2* telomeric silencing defect, this demonstrates that telomeric silencing is perturbed in the double mutant. This derepression appears to be specific for the telomeres because *hst3 hst4* mutant strains mate as well as wild-type. In contrast, *sir2* mutants are completely nonmating. The observed telomeric, but not *HM* loci, derepression may be attributable to competition for silencing factors, with

priority given to silencing the *HM* loci (Renauld et al. 1993), or may reflect overlapping but distinct specificities among the members of this gene family.

These experiments demonstrate that at least two of the *HST* family members have roles in transcriptional silencing, a third can participate in silencing processes, and that these genes can function at both the *HM* loci and telomeres.

hst3 hst4 *mutants arrest with undivided nuclei*

HST3 and *HST4* encode proteins of a subfamily distinct from Sir2p and Hst1p and are each other's closest relatives (Fig. 1B). *HST3* and *HST4* appear to encode redundant functions as double mutants have a number of phenotypes that are much less severe or lacking in *hst3* and *hst4* single mutants. A striking phenotype of *hst3 hst4* double mutant strains is the accumulation of large-budded cells with an undivided nucleus localized to the bud neck.

The cell cycle defects in the *hst3 hst4* double mutant suggest several possible explanations for the observed derepression of the telomeric regions in these strains. First, a similar accumulation of cells in G_2/M has been observed in a histone H4 mutant with multiple lysine to glutamine substitutions in the amino terminus (Megee et al. 1995). These mutants may mimic the constitutively acetylated, transcriptionally active state. Hypoacetylation of histones correlates with increased DNA compaction and thus transcriptional silencing (Lin et al. 1989). If like Sir2p, Hst3p and Hst4p are involved in modulating the levels of histone acetylation or deacetylation, *hst3 hst4* null mutations could cause increased levels of histone acetylation and thus increased transcription. A second possibility is that the longer G_2/M phase of the cell cycle may allow altered assembly of chromatin into a transcriptionally active state (Aparicio and Gottschling 1994).

The cell cycle defects could also be interpreted to suggest that loss of the silencing activities of *HST3* and *HST4* triggers a checkpoint that halts the cell at the G_2/M boundary. Cells unable to repair the problem would account for the decreased viability; those able to correct the problem would, after a delay, continue on into the next cycle. It is possible that a few cells might slip through the checkpoint and continue without properly correcting the defect, accounting for the nonviable cells remaining in the population. However, our data more strongly suggest that the accumulation of G_2/M phase cells results from a subpopulation that are ultimately inviable—most of the large-budded cells cannot form colonies and many of them fail to divide at all, continuing to grow (but not divide) until they eventually burst. What might send this subpopulation of *hst3 hst4* cells down this pathway of inexorable destruction? Possible primary defects we have considered, several of which have been observed previously in *sir* mutants, are DNA damage, improperly replicated DNA, incomplete chromosome condensation, or inability to properly assemble mitotic machinery.

Table 4. *Altered recombination in* hst *mutants*

Strain	Relevant genotype	Recombination frequency[a]
YCB692	*HST*$^+$	$1.7 \pm 0.45 \times 10^{-3}$
YCB693	*hst3*	$3.7 \pm 0.24 \times 10^{-3}$
YCB694	*hst4*	$2.2 \pm 0.33 \times 10^{-3}$
YCB695$^-$	*hst3 hst4*	$8.7 \pm 1.8 \times 10^{-3}$

[a]Calculated as Foa^R cells/total cells; mean of at least three independent determinations.

HST3 *and* HST4 *are required for genomic integrity*

Previously, *SIR* functions have been associated with chromosome stability and positioning. For example, *sir4* mutants lose chromosomes at a fourfold higher rate than wild type, and *sir3* and *sir4* mutants exhibit telomeric shortening and aberrant perinuclear localization (Palladino et al. 1993). In comparison, *hst3 hst4* double mutants display a 35-fold higher chromosome missegregation rate. Interestingly, the rate of chromosome nondisjunction is twice that of chromosome loss, suggesting a defect in sister chromatid separation during anaphase. It is unlikely that these phenotypes result simply from microtubule defects, because these strains show normal sensitivity to benomyl. Another possibility is disruption of centromeric function as mutations affecting the function of the centromere display a G_2/M delay and a high rate of chromosome fragment loss. We have observed aberrant mitotic spindles in the *hst3 hst4* mutant, consistent with aberrant chromosomal condensation or structure in the *hst3 hst4* mutant. It has been shown that cells displaying reduced chromosomal condensation before anaphase (Hirano et al. 1986) as well as other chromosome segregation defects (Doheny et al. 1993), lose chromosomes and exhibit a "Cut" phenotype in which the nucleus appears pinched in the middle; we observed the Cut phenotype in the *hst3 hst4* mutant (see Fig.4). In *Drosophila*, the *mus-101* mutant, like the *hst3 hst4* double mutant, is Ts lethal, has cell cycle and DNA repair defects, a chromosome segregation defect, and is defective in heterochromatin condensation (Gatti et al. 1983). Taken together, these results suggest that loss of silencing and/or chromosome condensation can lead to cell cycle, repair, and chromosome stability defects in diverse organisms.

Because mutations in *sir2* have been demonstrated to cause elevated levels of both mitotic and meiotic recombination in the rDNA repeats, we tested recombination frequencies in the *hst3 hst4* double mutant background. Using two different assays, we have shown that *hst3 hst4* strains exhibit a fivefold increase in general mitotic recombination. This is similar to the fourfold increase in mitotic recombination observed in *sir3* strains (Palladino et al. 1993) and in contrast to the *sir2* mutants whose effects on recombination appear specific for the highly repetitive rDNA (Gottlieb and Esposito 1989).

The accumulation of large budded cells with a G_2DNA content observed in *hst3 hst4* double mutant strains sug-

gests that a checkpoint may have been triggered leading to an arrest in G_2/M. In fact, the evidence described above points toward activation of a DNA-damage checkpoint. Thus, we tested whether the arrest caused by mutations in *hst3* and *hst4* was *RAD9* dependent. Although no decrease in viability was observed in the *hst3 hst4 rad9* triple mutant, these cells were hypersensitive to UV irradiation. These results suggest that the *HST* genes and *RAD9* are in parallel pathways that maintain genome integrity.

Finally, we have obtained evidence that chromosome maintenance is grossly defective in *hst1 hst2 hst3 hst4* strains, both in terms of chromosome number and structure. We have observed a number of defects in the electrophoretic karyotypes of these strains and their Ts^+ revertants (C. Brachmann, E. Cameron, and J. Boeke, unpubl.). We conclude that the Hst proteins are critical for maintaining genomic integrity.

Potential functions of the gene family

We propose that at least some of the new members of the *SIR2* gene family may be involved in the silencing of specific genomic regions, different from known silent loci. Each *HST* gene may have evolved specificity for one or more genomic regions; thus, Sir2p is essential for the "silencing complex" specific to the *HM* loci and telomeres. Although still somewhat speculative, there is evidence indicating that silencing complexes with altered specificities might include *SIR1*, *SIR3*, and *SIR4*. Recently, a semidominant mutant of *SIR4* encoding a carboxy-terminally truncated protein has been described that delays aging in yeast (Kennedy et al. 1995). This mutant has lost the ability to participate in silencing at the *HM* loci and telomeres, leading to their derepression. In addition, expression of only the carboxyl terminus of Sir4p extends the life span of wild-type cells, but reduces silencing at *HM* loci and telomeres. Together these experiments suggest that the carboxyl residues of Sir4p are responsible for recruiting the silencing complex to the *HM* loci and telomeres, and that when Sir4p can no longer recognize these regions, the complex is free to more tightly silence other parts of the genome. (An interesting requirement of this model is that silencing at the known loci be dominant to silencing at other regions of the genome.) We propose that Sir1p, Sir3p, and Sir4p may be components of a single silencing complex, the specificity of which is provided by interaction with a *SIR2* family member or members. Thus, if the *HST* genes are involved in silencing gene expression through altered chromatin structure, it is likely that additional, extensive genomic regions are silenced and structurally altered. Perturbations of such chromosomal structures may account for the genomic instability we have observed.

Our data show that *HST1* can function in transcriptional silencing at *HMR*, and that *hst3 hst4* mutants have a telomeric silencing defect. Moreover, *hst3 hst4* mutants display a number of phenotypes suggestive of defects in chromatin structure. Three general hypotheses may account for the observed results.

The first hypothesis linking the silencing functions of these genes to the mutant phenotypes is that the *HST* genes silence other genes; expression of these leads to a G_2/M delay and the other phenotypes described here. Such a scenario requires that these genes must normally function in a pathway other than vegetative growth (e.g., sporulation, diploid-specific growth, maintenance during starvation, pseudohyphal growth, or growth using unusual nutrients), because their expression in a logarithmically growing population leads to increased cell death.

A second possibility is that the *hst* mutant phenotypes are attributable to aberrant DNA replication. It is well established that silenced regions replicate late in S phase (McCarroll and Fangman 1988; Fangman and Brewer 1992; Ferguson and Fangman 1992). Loss of silencing caused by the deletion of the *HST* genes could be associated with an increased number of chromosomal regions replicating early. Alternatively, if the *HST* genes play a role in "silencing" replication origins after they have fired, there might be some overreplication in the mutant. Altered replication timing may lead to improperly replicated DNA, and ultimately impair the chromosome segregation machinery. The double mutant phenotypes are generally consistent with such a hypothesis, although we have no evidence for a large population of cells with incompletely replicated DNA. Thus, if aberrant replication occurs in the mutant, it may be a relatively subtle defect.

A third hypothesis is that loss of silencing caused by disruption of the *HST* genes results in a change in chromosomal structure significant enough to cause a G_2/M delay, chromosomal missegregation, and hyper-recombination. It is clear that silenced regions are structurally distinct from their transcriptionally active counterparts; silenced DNA is inaccessible to the UV-damage repair machinery (Terleth et al. 1989), nucleases (Loo and Rine 1994), and methylation by heterologous DNA methylation enzymes (Gottschling 1992; Singh and Klar 1992). Although there is no cytological evidence for heterochromatic regions in yeast, the correlation of heterochromatin with transcriptional repression in other organisms (PEV in *Drosophila*, X inactivation in mammals) and the importance of histones H3 and H4 in the process of silencing (Kayne et al. 1988; Johnson et al. 1990; Megee et al. 1990; Park and Szostak 1990; Thompson et al. 1994) suggest that the *HM* loci (and telomeres) in yeast may be defined functionally as heterochromatic. Gross alterations of chromosomal architecture, such as those that might result from derepression of a large number of normally silenced regions (as may be the case in the *hst* mutants), could have a deleterious effect on the cycling cell. The phenotypic similarities of the constitutively active H4 mutant (Megee et al. 1995) and the *hst3 hst4* mutant support the notion that global loss of silencing leads to cell cycle and chromosome segregation defects. Such altered chromatin might be recognized as aberrant by a cell cycle regulator, or the altered chromatin might

be damaged during attempts to segregate sister chromatids, or might present some physical impediment to proper segregation. Any one of these changes might lead to G_2/M arrest and ultimately, to cell death.

SIR2 *homologs from bacteria to humans*

Transcriptional silencing phenomena are observed in organisms from bacteria to humans and are important for such critical functions as bacterial virulence (Dagberg and Uhlin 1992) and X-chromosome inactivation (Migeon 1994). Although mechanisms of silencing and heterochromatin-mediated repression are arguably similar (Laurenson and Rine 1992; Weiler and Wakimoto 1995), little molecular overlap beyond histones has been observed previously. Our discovery of the *SIR2* family with homologs from *S. aureus, Arabidopsis thaliana, S. pombe, C. elegans, Mus musculus, R. norvegicus,* and *H. sapiens* suggests that these genes may fulfill an important conserved function. By extension, the existence of *HST*s in such diverse organisms also suggests that *SIR*-dependent silencing mechanisms may be used to regulate gene expression and genomic stability from simple to complex organisms.

Materials and methods

HST *gene identification and cloning*

HST1 was identified by several techniques including (1) a data base search in which the Sir2 protein sequence was searched against the translated GenBank and EMBL data bases using the BLAST network service and (2) low stringency blot hybridization. A region of homology to Sir2p was found within the 3′ flanking sequence of *NUF2*. A genomic clone containing the *HST1* gene (pGAD42C) and some sequence data were independently provided by C. Yan/T. Mélèse (Columbia University, NY) and G. Schlenstedt/P. Silver (Dana-Farber Cancer Institute, Boston, MA). An *HST1*-specific probe hybridizes to Olson λ clone 3083 on chromosome XV.

HST2 was originally identified in a two-hybrid screen designed to find interactors with TYA protein. The plasmid p113-2 was obtained from the library of partial *Sau*3A-digested yeast genomic DNA generously provided by P. Bartel and S. Fields (Chien et al. 1991), and contained the complete *HST2* gene fused six codons upstream of its ATG to the *GAL4* DNA-binding domain. Subsequent screens of a genomic library (C. Connelly and P. Hieter, unpubl.) allowed isolation of plasmid pCAR135 containing intact *HST2*. An *HST2*-specific probe hybridized to Olson cosmid 9901 on chromosome XVI.

By aligning Sir2p, *K. lactis* Sir2p, *S. aureus* Sir2p, and Hst2p, we defined conserved sequence motifs, allowing degenerate primer design (Fig. 1A). To identify *HST3*, we used degenerate PCR on genomic DNA from *sir2 hst1 hst2* strain YCB240 with primers JB710 (GGNRTNCCNGAYTTY[A/C]G) and JB708 (RTC[A/G/T]ATRTTYTGNGTRTA). Touchdown PCR conditions were as follows: 1 min at 94°C, 30 sec at 54°C, 30 sec at 72°C] for 2 cycles, 1 min at 94°C, 30 sec at 50°C, 30 sec at 72°C for 2 cycles, 1 min at 94°C, 30 sec at 46°C, 30 sec at 72°C for 2 cycles, 1 min at 94°C, 30 sec at 42°C, 30 sec at 72°C for 2 cycles, 1 min at 94°C, 30 sec at 38°C, 30 sec at 72°C for 2 cycles, 1 min at 94°C, 30 sec at 48°C, 30 sec at 72°C for 25 cycles, 5 min at 72°C. The ~240-bp band was gel purified, ethanol precipitated, and treated with T4 polymerase to create a blunt end (a process referred to as blunting) and cloned into pBSII SK+ (Stratagene) linearized with *Eco*RV. The insert fragment from one subclone (pCAR187) was used to probe a genomic library (C. Connelly and P. Hieter, unpubl.). Three plasmids with overlapping inserts (pCAR192, pCAR195, and pCAR196) were obtained. The *HST3* probe hybridized to Olson λ clone 4170 on chromosome XV.

To identify *HST4*, we performed degenerate PCR as described above on genomic DNA from strain YCB388 (*sir2 hst1 hst2 hst3*) and cloned a 240-bp product. The *HST4* probe hybridizes to Olson λ clones 4040 and 6708 on chromosome IV.

DNA sequencing

DNA sequences were determined on both strands for *HST1, HST2,* and *HST3* using a recently developed in vitro transposon-mediated sequencing technique (Devine and Boeke 1994) in conjunction with manual or ABI automated sequencing. *HST1* and *HST3* were sequenced using the artificial trimethoprim-resistance transposon AT-2 (Devine and Boeke 1994), which was inserted into the plasmids pGAD42C and pCAR206 carrying 2.2-kb *HST1* and 1.9-kb *HST3* inserts, respectively. *HST2* was sequenced using a progenitor artificial transposon closely resembling AT-2 but with slightly different termini, constructed by PCR, and integrated into pCAR143, carrying a 4.5-kb *HST2* insert. Approximately 500–5000 independent artificial transposon recombinants were generated for each plasmid target using Ty1–VLP integrase in vitro. Ampicillin/trimethoprim-resistant recombinants (30–60 per plasmid target) were screened by restriction mapping to identify transposon insertions in the respective *HST* inserts. Miniprep DNA from recombinants chosen for sequence analysis were treated with 10 μg/ml of RNase A for 30 min at 37°C, phenol/chloroform extracted, ethanol precipitated, and resuspended in water at a concentration of ≥200 μg/ml immediately before sequencing.

In the case of *HST2*, 26 transposon recombinants were sequenced manually using Sequenase T7 polymerase (U.S. Biochemical) according to the manufacturers instructions. In addition to the transposon-specific primers (SD110 and SD111), the T3 and T7 primer sites flanking the insert were also used to recover the terminal sequences. For *HST1* and *HST3*, a smaller number of premapped, optimally spaced AT-2 transposon insertions were sequenced with *Taq* polymerase (Perkin-Elmer) using Prizm kit dye-terminator cycle sequencing in conjunction with an Applied Biosystems 373A Stretch automated sequencer. Sequencing reactions intiated from eight AT-2 insertions (using primers SD118 and SD119) plus the T3 and T7 primers yielded the complete *HST1* sequence. Reactions from 12 transposon insertions (plus the T3 and T7 sites) yielded the complete *HST3* sequence. Sequences were assembled and analyzed using Sequencher software (Genecodes, Inc., Ann Arbor, MI) for the Macintosh computers.

Sequence and data base analysis

Multiple sequence alignments were performed using the PILEUP program of the GCG software package (University of Wisconsin, Madison, WI) with preset options, adjusted as described in Figure 1. Homologs of *SIR2* from *S. aureus* (*SaSIR2*, M32103) and *R. norvegicus* (*RnSIR2*, D37934) were sequenced as flanking DNA of the *lac* operon (Oskouian and Stewart 1990) and the 5E5 antigen cDNA (Yoshimura et al. 1990) respectively, allowing their identification through TBLASTN data base searches. The *SaSIR2* sequence was corrected by insertion of a single C at position 692 based on sequencing of the region cor-

responding to nucleotides 645–941, amplified by PCR on a *S. aureus* colony. Although the *SaSIR2* homolog sequence is complete, the *RnSIR2* sequence probably is not. Because the cDNA sequence encodes the homolog on the minus strand upstream of and slightly overlapping the 5E5 antigen, it is unclear where the *RnSIR2* ORF begins. For the alignment we truncated this sequence at its amino terminus, guided by similarities to the human sequence. The partial *H. sapiens* homolog (*HsSIR2*) sequence was assembled into a contig encoding a single ORF from expressed sequence tag (EST) data base sequences (H14246, R24561, F11858, T66100, R15236, Z42780, T81280, T83544, R25838, R13142, H11816, R56596, F00550, R16487, R07921, H06578, and H06548) and additional sequencing of T66100 cDNA. The *K. lactis* homolog sequence was reported previously (Chen and Clark-Walker 1994). The *C. elegans* genome sequencing effort recently identified two tightly linked *SIR2* homologs (Z50177). Additional ESTs from *A. thaliana* and mouse were also found (not shown). Pairwise comparisons were performed using the GAP program of the GCG software package. Data base searches were performed at the National Center for Biotechnology Instruction (NCBI) using the BLAST network service. Some of the homologous EST sequences were identified through the XREF project (Bassett et al. 1995).

Strains, media, and disruption mutations

Yeast strains are derived from strains YPH499, 500 and 501 (Sikorski and Hieter 1989), FY2 (Winston et al. 1995), or W303 and are described in Table 1. All media used were as described (Rose et al. 1990).

Multiple deletion/disruption mutations were analyzed. The following alleles represent partial deletion/disruption mutations: *hst1Δ2::LEU2*, *hst2Δ1::TRP1*, *hst4Δ1::URA3*, *hst4Δ1::TRP1*. The following alleles represent complete deletion/disruption mutations (in which the entire *HST* ORF is replaced): *hst1Δ3::TRP1*, *hst2Δ2::TRP1*, *hst3Δ3::HIS3*, *hst3Δ3::TRP1 sir2Δ2::TRP1*. In no case tested did the phenotypes of partial or full deletion alleles differ; details will be published elsewhere.

Plasmids

Plasmids for overexpression studies were constructed in the *ADE2* 2μ plasmid pJK204 (Keeney et al. 1995) or in the *URA3* 2μ plasmid YEp352 (Hill et al. 1986). For pLP317, the *SIR2* overexpression plasmid, the 2.7-kb *Bst*NI fragment containing the gene was treated with VENT DNA polymerase (New England BioLabs) and subcloned into YEp352 digested with *Sma*I. The *HST1* overexpression plasmid pLP316 was made by subcloning the 2.2-kb *Sac*I fragment containing *HST1* from pGAD42C into *Sac*I-digested YEp352. pCAR143 (used for sequence analysis of *HST2*) is pCAR135 cut with *Xba*I and recircularized. The *HST2* overexpression plasmid pCAR172 was constructed by subcloning the *Xba*I–*Cla*I fragment containing *HST2* from pCAR143 into pJK204, which had been digested with *Cla*I and *Nhe*I. For pCAR211, the *HST3* overexpression plasmid, the 3.7-kb *Hin*dIII fragment from pCAR192 was first subcloned into pRS415 making pCAR202. pCAR202 was digested with *Sal*I, treated with Klenow to create a blunt end, and then digested with *Xba*I. The resulting 3.7-kb fragment containing *HST3* was ligated into pJK204, which had been linearized with *Cla*I, blunted with Klenow, and then digested with *Nhe*I. Plasmid pCAR206 used for the sequence analysis of *HST3* was constructed by cloning the 1.9-kb *Pst*I–*Hpa*I fragment containing *HST3* from pCAR202 into pMOB (Strathmann et al. 1991) digested with *Pst*I and *Ecl*136II.

Quantitative mating analysis with high copy HST *genes*

Quantitative matings with YEp352 (*URA3* 2μ), pLP316 (*HST1 URA3* 2μ), pLP317 (*SIR2 URA3* 2μ) transformants of *sir2* strains LPY11 and LPY1393 were performed essentially as described by Sprague (1991). The assays to evaluate $SUP3_{am}$ expression by measuring $trp1_{am}$ suppression were performed by diluting saturated overnight cultures of LPY1539, growing in SC–Ura to an OD_{600} of 1.0, and making serial fivefold dilutions. Three microliters of each dilution were spotted onto plates to select for plasmid only (SC–Ura plates) and for $trp1_{am}$ suppression in the presence of plasmid (SC–Trp–Ura plates).

Chromosome loss rate determination

Chromosome loss assays were performed essentially as described, using the chromosome fragments "*CEN3* left" and "*RAD2* distal" (Spencer et al. 1990). Diploid strains harboring a fragment were taken from plates selective for the fragment, resuspended in H_20, briefly sonicated, and plated at a density of 200 per plate onto supplemented minimal plates including 6 μg/ml of adenine (to enhance red pigment formation in *ade2* strains). After 5 days at 30°C, these plates were incubated further at 4°C for > 1 week before scoring. Loss rates were determined by counting the number of red:pink half-sectored colonies (1:0 events) and the number of red:white half-sectored colonies (2:0 events) and dividing by the number of fully pink colonies (containing one chromosome fragment).

Flow cytometry and microscopy

For flow cytometric analysis, approximately 1×10^6 cells from yeast strains grown to early- to mid-log phase (OD_{600} = 0.3–0.8) were collected and fixed overnight at 4°C in 70% ethanol, 0.2 M Tris-Cl (pH 7.6). After two washes, cells were resuspended in 0.2 ml of 1 μg/ml RNase A, 0.2 M Tris-HCl (pH 7.6) and incubated at 37°C for 4–6 hr. Cells were then washed twice, resuspended in 1 ml of 0.2 M Tris-HCl (pH 7.6) containing 3 μg/ml of propidium iodide (Sigma), and incubated for 1–5 days at 4°C. Flow cytometric analysis was performed on a Coulterepics 752 apparatus with a gain of 10 and high voltage of 935 V. Propidium iodide-stained cells were excited with 400 mW of 488 nm light and integrated red (≥590 nm) fluorescence was recorded.

For nuclear morphology determination, early- to mid-log phase cells were collected. Nuclei and microtubules were stained and visualized as described (Doheny et al. 1993). Phase contrast microscopy was performed on live or fixed cells.

Viability determination

Individual log phase cells grown in liquid YPD (OD_{600} = 0.5) were micromanipulated on YPD plates and grown at 30°C and assessed for colony formation. For determination of viability of large-budded cells, only those cells in which the daughter cell was >50% the size of the mother cell were micromanipulated.

Acknowledgments

We thank M. Goebl for pointing out limited homology between *HST2* and *SIR2*, R. Sternglanz for piquing our interest, and J. Rine and P. Hieter for uplifting discussions. We gratefully acknowledge M. Derbyshire and J. Strathern for communication of data regarding their independent discovery of the *HST* gene family prior to publication. C.B.B. and J.D.B. thank R. Brachmann for support, Toby for patience, D. Bassett Jr. for XREFdb expertise, and J. Fluke for assistance with FACScan analysis.

J.M.S. and L.P. thank C. Yan and T. Mélèse for their important early contributions. Sequence analysis was supported by a sponsored research agreement with the Perkin-Elmer Corporation, Applied Biosystems Division, to S.E.D. and J.D.B. Supported in part by a National Science Foundation (NSF) Predoctoral Fellowship to C.B.B., an American Cancer Society (ACS) Postdoctoral Fellowship to S.E.D., funding from the Pew Charitable Trust and the NSF to L.P., and an ACS Faculty Research Award and National Institutes of Health (NIH) grant to J.D.B.

The publication costs of this article were defrayed in part by payment of page charges. This article must therefore be hereby marked "advertisement" in accordance with 18 USC section 1734 solely to indicate this fact.

References

Allshire, R.C., J.-P. Javerzat, N.J. Readhead, and G. Cranston. 1994. Position effect variegation at fission yeast centromeres. *Cell* **76:** 157–169.

Aparicio, O.M. and D.E. Gottschling. 1994. Overcoming telomeric silencing—A *trans*-activator competes to establish gene expression in a cell cycle-dependent way. *Genes & Dev.* **8:** 1133–1146.

Aparicio, O.M., B.L. Billington, and D.E. Gottschling. 1991. Modifiers of position effect are shared between telomeric and silent mating-type loci in S. cerevisiae. *Cell* **66:** 1279–87.

Bassett, D.E. Jr., M.S. Boguski, F. Spencer, R. Reeves, M. Goebl, and P. Hieter. 1995. Comparative genomics, genome cross-referencing and XREFdb. *Trends Genet.* **11:** 372–373.

Bell, S.P., R. Kobayashi, and B. Stillman. 1993. Yeast origin recognition complex functions in transcription silencing and DNA replication [see comments]. *Science* **262:** 1844–1849.

Braunstein, M., A.B. Rose, S.G. Holmes, C.D. Allis, and J.R. Broach. 1993. Transcriptional silencing in yeast is associated with reduced nucleosome acetylation. *Genes & Dev.* **7:** 592–604.

Buchman, A.R., W.J. Kimmerly, J. Rine, and R.D. Kornberg. 1988. Two DNA-binding factors recognize specific sequences at silencers, upstream activating sequences, autonomously replicating sequences, and telomeres in Saccharomyces cerevisiae. *Mol. Cell. Biol.* **8:** 210–25.

Butner, K. and C.W. Lo. 1986. Modulation of *tk* expression in mouse pericentromeric heterochromatin. *Mol. Cel. Biol.* **6:** 4440–4449.

Chen, X.-J. and G.D. Clark-Walker. 1994. *sir2* mutants of *Kluyveromyces lactis* are hypersensitive to DNA-targeting drugs. *Mol. Cell. Biol.* **14:** 4501–4508.

Chien, C.T., P.L. Bartel, R. Sternglanz, and S. Fields. 1991. The two-hybrid system: A method to identify and clone genes for proteins that interact with a protein of interest. *Proc. Natl. Acad. Sci.* **88:** 9578–9582.

Cockell, M., F. Palladino, T. Laroche, G. Kyrion, C. Liu, A.J. Lustig, and S.M. Gasser. 1995. The carboxy termini of Sir4 and Rap1 affect Sir3 localization—Evidence for a multicomponent complex requiredfor yeast telomeric silencing. *J. Cell Biol.* **129:** 909–924.

Dagberg, B. and B.E. Uhlin. 1992. Regulation of virulence-associated plasmid genes in enteroinvasive Escherichia coli. *J. Bacteriol.* **174:** 7606–7612.

Dani, G.M. and V.A. Zakian. 1983. Mitotic and meiotic stability of linear plasmids in yeast. *Proc. Natl. Acad. Sci.* **80:** 3406–3410.

Derbyshire, M.K., K.G. Weinstock, and J.N. Strathern. 1995. *HST1*, a new member of the *SIR2* fanily of genes. *Yeast* (in press).

Devine, S.E. and J.D. Boeke. 1994. Efficient integration of artificial transposons into plasmid targets *in vitro*: A useful tool for DNA mapping, sequencing and genetic analysis. *Nucleic Acids Res.* **22:** 3765–3772.

Doheny, K.F., P.K. Sorger, A.A. Hyman, S. Tugendreich, F. Spencer, and P. Hieter. 1993. Identification of essential components of the *S. cerevisiae* kinetochore. *Cell* **73:** 761–774.

Fangman, W.L. and B.J. Brewer. 1992. A question of time: Replication origins of eukaryotic chromosomes. *Cell* **71:** 363–366.

Ferguson, B.M. and W.L. Fangman. 1992. A position effect on the time of replication origin activation in yeast. *Cell* **68:** 333–339.

Foss, M., F.J. McNally, P. Laurenson, and J. Rine. 1993. Origin recognition complex (ORC) in transcriptional silencing and DNA replication in S. cerevisiae. *Science* **262:** 1838–1844.

Gatti, M., D.A. Smith, and B.S. Baker. 1983. A gene controlling condensation of heterochromatin in Drosophila melanogaster. *Science* **221:** 83–85.

Gerring, S.L., F. Spencer, and P. Hieter. 1990. The *CHL1* (*CTF1*) gene product of *Saccharomyces cerevisiae* is important for chromosome transmission and normal cell cycle progression in G2/M. *EMBO J.* **9:** 4347–4358.

Gottlieb, S. and R.E. Esposito. 1989. A new role for a yeast transcriptional silencer gene, SIR2, in regulation of recombination in ribosomal DNA. *Cell* **56:** 771–776.

Gottschling, D.E. 1992. Telomere-proximal DNA in Saccharomyces cerevisiae is refractory to methyltransferase activity in vivo. *Proc. Natl. Acad. Sci.* **89:** 4062–4065.

Gottschling, D.E., O.M. Aparicio, B.L. Billington, and V.A. Zakian. 1990. Position effect at S. cerevisiae telomeres: Reversible repression of Pol II transcription. *Cell* **63:** 751–762.

Guillen, N., M. Amar, and L. Hirschbein. 1985. Stabilized non-complementing diploids (Ncd) from fused protoplast products in *B. Subtilis. EMBO J.* **4:** 1333–1338.

Hecht, A., T. Laroche, S. Strahl-Bolsinger, S.M. Gasser, and M. Grunstein. 1995. Histone H3 and H4 N-termini interact with SIR3 and SIR4 proteins: A molecular model for the formation of heterochromatin in yeast. *Cell* **80:** 583–592.

Hieter, P., C. Mann, M. Snyder, and R.W. Davis. 1985. Mitotic stability of yeast chromosomes: A colony color assay that measures nondisjunction and chromosome loss. *Cell* **40:** 381–392.

Hill, J.E., A.M. Myers, T.J. Koerner, and A. Tzagoloff. 1986. Yeast/E.coli shuttle vectors with multiple unique restriction sites. *Yeast* **2:** 163–167.

Hirano, T., S. Funahashi, T. Uemura, and N. Yanagida. 1986. Isolation and characterization of Schizosaccharomyces cut mutants that block nuclear division but not cutokenesis. *EMBO J.* **5:** 2973–2979.

Johnson, L.M., P.S. Kayne, E.S. Kahn, and M. Grunstein. 1990. Genetic evidence for an interaction between SIR3 and histone H4 in the repression of the silent mating loci in Saccharomyces cerevisiae. *Proc. Natl. Acad. Sci.* **87:** 6286–6290.

Kayne, P.S., U.J. Kim, M. Han, J.R. Mullen, F. Yoshizaki, and M. Grunstein. 1988. Extremely conserved histone H4 N terminus is dispensable for growth but essential for repressing the silent mating loci in yeast. *Cell* **55:** 27–39.

Keeney, J.B., K.B. Chapman, V. Lauermann, D.F. Voytas, S.U. Åström, U. von Pawel-Rammingen, A. Byström, and J.D. Boeke. 1995. Multiple molecular determinants for retrotransposition in a primer tRNA. *Mol. Cell. Biol.* **15:** 217–226.

Kennedy, B.K., N.R. Austriaco Jr., J. Zhang, and L. Guarente. 1995. Mutation in the silencing gene SIR4 can delay aging in

S. cerevisiae. *Cell* **80:** 485–496.

Laman, H., D. Balderes, and D. Shore. 1995. Disturbance of normal cell cycle progression enhances the establishment of transcriptional silencing in *Saccharomyces cerevisiae*. *Mol. Cell. Biol.* **15:** 3608–3617.

Laurenson, P. and J. Rine. 1992. Silencers, silencing, and heritable transcriptional states. [Review]. *Microbiol. Rev.* **56:** 543–560.

Lin, R., J.W. Leone, R.G. Cook, and C.D. Allis. 1989. Antibodies specific to acetylated histones document deposition- and transcription-related histone acetylation in *Tetrahymena*. *J. Cell Biol.* **108:** 1577–1588.

Loo, S. and J. Rine. 1994. Silencers and domains of generalized repression. *Science* **264:** 1768–1771.

———. 1995. Silencing and heritable domains of gene expression. *Annu. Rev. Cell Biol. Dev.* **11:** 519–548.

Mahoney, D.J. and J.R. Broach. 1989. The HML mating-type cassette of Saccharomyces cerevisiae is regulated by two separate but functionally equivalent silencers. *Mol. Cell. Biol.* **9:** 4621–4630.

McCarroll, R.M. and W. Fangman. 1988. Time of replication of yeast centromeres and telomeres. *Cell* **54:** 505–513.

Megee, P.C., B.A. Morgan, B.A. Mittman, and M.M. Smith. 1990. Genetic analysis of histone H4: Essential role of lysines subject to reversible acetylation. *Science* **247:** 841–845.

Megee, P.C., B.A. Morgan, and M.M. Smith. 1995. Histone H4 and the maintenance of genome integrity. *Genes & Dev.* **9:** 1716–1727.

Micklem, G., A. Rowley, J. Harwood, K. Nasmyth, and J.F. Diffley. 1993. Yeast origin recognition complex is involved in DNA replication and transcriptional silencing. *Nature* **366:** 87–89.

Migeon, B. 1994. X-chromosome inactivation: Molecular mechanisms and genetic consequences. *Trends Genet.* **10:** 230–235.

Moretti, P., K. Freeman, L. Coodly, and D. Shore. 1994. Evidence that a complex of sir proteins interacts with the silencer and telomere binding protein rap1. *Genes & Dev.* **8:** 2257–2269.

Nimmo, E.R., G. Cranston and R.C. Allshire. 1994. Telomere-associated chromosome breakage in fission yeast results in variegated expression of adjacent gene. *EMBO J.* **13:** 3801–3811.

Oskouian, B. and G.C. Stewart. 1990. Repression and catabolite repression of the lactose operon of *Staphylococcus aureus*. *J. Bacteriol.* **172:** 3804–3812.

Paetkau, D.W., J.A. Riese, W.S. MacMorran, R.A. Woods, and R.D. Gietz. 1994. Interaction of the yeast RAD7 and SIR3 proteins: Implications for DNA repair and chromatin structure. *Genes & Dev.* **8:** 2035–2045.

Palladino, F., T. Laroche, E. Gilson, A. Axelrod, L. Pillus and S.M. Gasser. 1993. SIR3 and SIR4 proteins are required for the positioning and integrity of yeast telomeres. *Cell* **75:** 543–555.

Park, E.C. and J.W. Szostak. 1990. Point mutations in the yeast histone H4 gene prevent silencing of the silent mating type locus HML. *Mol. Cell. Biol.* **10:** 4932–4934.

Pillus, L. and J. Rine. 1989. Epigenetic inheritance of transcriptional states in *S. cerevisiae*. *Cell* **59:** 637–647.

Renauld, H., O.M. Aparicio, P.D. Zierath, B.L. Billington, S.K. Chhablani, and D.E. Gottschling. 1993. Silent domains are assembled continuously from the telomere and are defined by promoter distance and strength, and by SIR3 dosage. *Genes & Dev.* **7:** 1133–1145.

Rose, M.D., F. Winston, and P. Hieter. 1990. *Methods in yeast genetics. A laboratory course manual*. Cold Spring Harbor Laboratory Press, Cold Spring Harbor, New York.

Schaeffer, P., B. Cami, and R.D. Hotchkiss. 1976. Fusion of bacterial protoplasts. *Proc. Natl. Acad. Sci.* **73:** 2151–2155.

Schnell, R. and J. Rine. 1986. A position effect on the expression of a tRNA gene mediated by the SIR genes in Saccharomyces cerevisiae. *Mol. Cell. Biol.* **6:** 494–501.

Shei, G.J. and J.R. Broach. 1995. Yeast silencers can act as orientation-dependent gene inactivation centers that respond to environmental signals. *Mol. Cell. Biol.* **15:** 3496–3506.

Shero, J.H., M. Koval, F. Spencer, R.E. Palmer, P. Hieter, and D. Koshland. 1991. Analysis of chromosome segregation in Saccharomyces cerevisiae. *Methods Enzymol.* **194:** 749–773.

Shore, D. 1994. RAP1—A protean regulator in yeast. *Trends Genet.* **10:** 408–412.

Sikorski, R.S. and P. Hieter. 1989. A system of shuttle vectors and yeast host strains designed for efficient manipulation of DNA in Saccharomyces cerevisiae. *Genetics* **122:** 19–27.

Singh, J. and A.J. Klar. 1992. Active genes in budding yeast display enhanced in vivo accessibility to foreign DNA methylases: A novel in vivo probe for chromatin structure of yeast. *Genes & Dev.* **6:** 186–196.

Spencer, F., S.L. Gerring, C. Connelly, and P. Hieter. 1990. Mitotic chromosome transmission fidelity mutants in Saccharomyces cerevisiae. *Genetics* **124:** 237–249.

Sprague, G.F. 1991. Assay of yeast mating reaction. *Methods Enzymol.* **194:** 77–93.

Strathmann, M., B.A. Hamilton, C.A. Mayeda, M.I. Simon, E.M. Meyerowitz, and M.J. Palazzolo. 1991. Transposon-facilitated DNA sequencing. *Proc. Natl. Acad. Sci.* **88:** 1247–1250.

Sussel, L. and D. Shore. 1991. Separation of transcriptional activation and silencing functions of the *RAP1*-encoded repressor/activatior protein 1: Isolation of viable mutants affecting both silencing and telomere length. *Proc. Natl. Acad. Sci.* **88:** 7749–7753.

Sussel, L., D. Vannier, and D. Shore. 1993. Epigenetic switching of transcriptional states: Cis- and trans-acting factors affecting establishment of silencing at the *HMR* locus in *Saccharomyces cerevisiae*. *Mol. Cell. Biol.* **13:** 3919–3928.

Terleth, C., C.A. van Sluis, and P. van de Putte. 1989. Differential repair of UV damage in *Saccharomyces cerevisiae*. *Nucleic Acids Res.* **17:** 4433–4439.

Thompson, J.S., X.F. Ling, and M. Grunstein. 1994. Histone h3 amino terminus is required for telomeric and silent mating locus repression in yeast. *Nature* **369:** 245–247.

Weiler, K.S. and B.T. Wakimoto. 1995. Heterochromatin and gene expression in *Drosophila*. *Ann. Rev. Genet.* **29:** 577–605.

Weinert, T.A. and L.H. Hartwell. 1988. The RAD9 gene controls the cell cycle response to DNA damage in Saccharomyces cerevisiae. *Science* **241:** 317–322.

Weinert, T.A., G.L. Kiser, and L.H. Hartwell. 1994. Mitotic checkpoint genes in budding yeast and the dependence of mitosis on DNA replication and repair. *Genes & Dev.* **8:** 652–665.

Winston, F., C. Dollard, and S.L. Ricupero-Hovasse. 1995. Construction of a set of convenient *Saccharomyces cerevisiae* strains that are isogenic to S288C. *Yeast* **11:** 53–55.

Wright, J.H., D.E. Gottschling, and V.A. Zakian. 1992. *Saccharomyces* telomeres assume a non-nucleosomal chromatin structure. *Genes & Dev.* **6:** 197–210.

Yoshimura, K., K. Akagawa, Y. Nishimura, and K. Uyemura. 1990. A monoclonal antibody 5E5 recognizes an intranuclear antigen selectively present in a subpopulation of the neurons. *Brain Res.* **509:** 161–164.

The SIR2 gene family, conserved from bacteria to humans, functions in silencing, cell cycle progression, and chromosome stability.

C B Brachmann, J M Sherman, S E Devine, et al.

Genes Dev. 1995, **9:**
Access the most recent version at doi:10.1101/gad.9.23.2888